Dalton Transactions

PAPER

View Article Online
View Journal | View Issue

Cite this: *Dalton Trans.*, 2016, **45**, 2102

Metal carbonyl complexes of phosphaamidines. Coordinative integrity detected in *C*-amino(λ^3,σ^2)-phosphaalkene isomers coordinated through *n*(P) HOMO−1 donor orbitals†

Jason D. Masuda[a] and René T. Boeré*[b]

Received 1st September 2015,
Accepted 1st October 2015

DOI: 10.1039/c5dt03393d

www.rsc.org/dalton

Metal(0) complexes L(Cr,Mo,W)$(CO)_5$ have been prepared from 1,3-bis(2,6-diisopropylphenyl)-2-(4-methylphenyl)-3-aza-1(λ^3,σ^2)-phosphapropene and 1,3-bis(2,6-diisopropylphenyl)-2-(4-methoxyphenyl)-3-aza-1(λ^3,σ^2)-phosphapropene using standard methods. Full characterization of four products and crystal structures of these complexes as well as the methoxyphenyl-phosphapropene are reported. The ligands coordinate κ*P*, common for simple phosphaalkenes, despite the strongly-perturbing amino substitution at the double bond C atoms. Analyses of the NMR and vibrational spectroscopic data reveal that the complexes have very similar character to similarly-coordinated phosphaalkenes, with strong σ-donor character. The presence of some net π-interactions (acceptor or donor) is indicated by structures in which the ligands coordinate fully eclipsed with the M−CO groups. The synthetic and structural results have been augmented by B3PW91/LANL2DZ calculations that reproduce the structures of the Cr complexes accurately. The calculated vibrational spectra are used to confirm the assignment of the ν(C≡O) vibrational data. Detailed orbital interaction diagrams based on DFT calculations are reported for the title complexes as well as for the $Cr(CO)_5$ complex of Mes−P=CPh_2. The electronic absorption spectra of the title complexes have intense low-energy absorptions ranging from 24 500 to 25 300 cm^{-1}, which can be interpreted qualitatively using the DFT results.

Introduction

Interest in P(III) monophosphaamidine‡ chemistry has increased greatly in recent years after languishing for a long time since the initial discoveries by Issleib *et al.* at the dawn of phosphorus–carbon multiple bond chemistry.[1,2] In 2004 we published the first modern results on an *N*,*P*-disubstituted aryl phosphaamidine **1** (Chart 1) and demonstrated that it could be deprotonated with lithium and potassium reagents; crystal structures of the neutral phosphaamidine and the two metal derivatives were reported.[3] Song *et al.* reported the first phosphorus derivative of formamidine **2** (H on the C backbone) including a lithium complex with a structure similar to ours (and also provided a nice survey of much of the older literature).[4] Thereafter, Li *et al.* reported the synthesis of a new

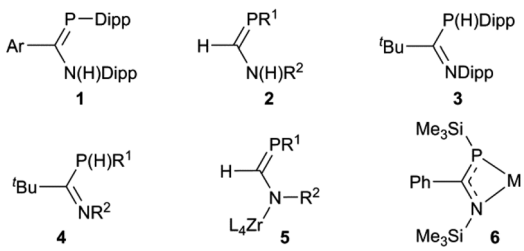

Chart 1

[a]*Department of Chemistry, Saint Mary's University, Halifax, Nova Scotia, Canada, B3H 3C2*
[b]*Department of Chemistry and Biochemistry, University of Lethbridge, Lethbridge, Alberta, Canada, T1K 3M4. E-mail: boere@uleth.ca; Fax: +403-329-2057; Tel: +403-329-2045*

†Electronic supplementary information (ESI) available: Thermal ellipsoid plots of isostructural **11a**, **12**; table of P=C bond distances from the CSD, with structure diagrams; DFT structure of **10** and overlay with X-ray geometry; graphs of correlations between out-of-plane distances and dihedral angles with P=C distances; additional FTIR data; refined disorder model of **11b**, crystal and refinement parameters; Cartesian coordinates of DFT structures. CCDC 1421316–1421320. For ESI and crystallographic data in CIF or other electronic format see DOI: 10.1039/c5dt03393d

‡Phosphorus can substitute for one or both nitrogen atoms in the organic amidine functional group where the pnictogens are normally in the +3 oxidation state, resulting in 1(λ^3,σ^2)-monophosphaamidines or 1,3(λ^3,σ^2)-diphosphaamidines, which can then form the corresponding phosphaamidinates if there is at least one ionisable hydrogen atom. Alternatively, phosphorus in the +5 oxidation state can replace the backbone carbon atom, resulting in inorganic 2(λ^5,σ^2)-phosphaamidines and amidinates;[77] the latter modality has previously been named "fosfam".

exemplar **3** with ^{t}Bu on the backbone with crystal structures of Li, K and Tl derivatives.[5] Most recently, van Dijk *et al.* have reported several additional examples of such phosphaamidines **4**, all with backbone ^{t}Bu and various aromatic groups on N and P, as well as some lithium and rhodium complexes.[6] In parallel with these reports using conventional synthesis followed by complexation of deprotonated anions, Waterman has reported the elegant assembly of phosphaformamidinate complexes **5** from precursors coordinated to a zirconium scorpionate framework.[7–9] His group also recently reported the first example of a coordinated arsaformamidinate.[10] Several examples of the NCP unit **6**, *i.e.* 1,3-azaphosphaallyls of Mg, Ca, Sr, Ba, Li and Sn have been prepared by silyl migration (the N and P substituents are thereby always a TMS group).[11,12] This recent work follows on a more extensive exploration by many workers on metal complexes of tri-substituted analogues which lack an ionisable H atom and hence tend to be prepared exclusively in one tautomeric form,[13–18] including conventional phosphaalkenes,[19–31] phosphacumulenes,[32–40] alkoxy- ("Becker") phosphaalkenes R′PC(R)OR″,[41–44] aminophosphaalkenes R′PC(R)NR″$_2$ (ref. 45–48) and diaminophosphaalkenes R′PC(NR″$_2$)$_2$.[49] The latter three types are sometimes referred to as 'polarized phosphaalkenes' or as having 'reverse electron demand' compared to R′P═CR$_2$ and R′P═CRR″.[50,51]

Our entry into this field of research was from organic amidinates which can be tuned with a wide variety of substituents R, R′ and R″ in the R′NC(R)NR″ positions, and can be synthesised by many routes, of which the deprotonation of R′NC(R)-NHR″ is the most common and the most versatile.[52] Thus after preparing a series of amidines **7** using the bulky 2,6-diisopropylphenyl (Dipp) group for R′ and R″ with R = aryl, methyl or trifluoromethyl on the carbon backbone (see Scheme 1),[53–55] our aim is to prepare and investigate phosphaamidines that are exact molecular copies exchanging only N for P.

We also reported (Scheme 1) that amidines **7** react with Mo(CO)$_6$ under thermal conditions to give the η^6-aryl coordinated Mo(CO)$_3$ complexes **8** as the only stable metal derivatives (that is, zero-valent Mo prefers the electron-rich aromatic ring to N atom coordination).[53,54] By contrast, less-bulky amidines react under similar conditions to afford L$_4$M$_2$ "lantern" amidinate complexes *via* a redox reaction.[56] Once the corresponding phosphaamidines **1** were in hand, we wanted to know how these would react with M(CO)$_6$. Unlike common R$_3$P ligands, **1** have a choice between side-on (κ^2*P*,*C*) coordination of the P═C double bond and the *n*(P) orbital (κ*P*).

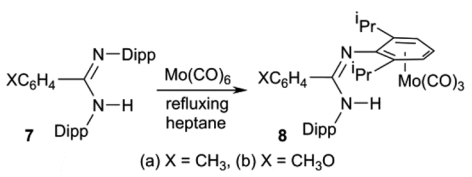

Scheme 1

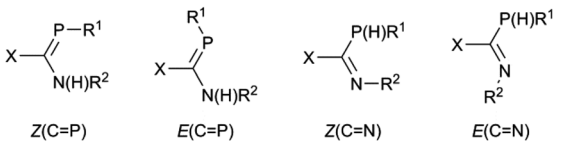

Scheme 2

A second motivation for this study relates to the propensity of **1** to isomerize in solution. This issue will be the subject of a separate publication,[57] but briefly it is found that for some combinations of substituents X, R^1 and R^2, pure samples dissolve to give up to four different interchanging solution species, and there is evidence that these include the expected *E*/*Z* isomers at the double bonds as well as *C*-amino-(λ^3,σ^2)-aminophosphaalkene/*C*-(λ^3,σ^3)-phosphinoimine tautomers (Scheme 2). It was thus of interest to see what effect coordination to metals will have on species prone to such an isomerization; LM(CO)$_5$ complexes of Cr, Mo and W have an extensive history for the stabilization of reactive low-coordinated main group compounds.[19–49]

Synthesis of LM(CO)$_5$ complexes

The phosphaamidines **9** were synthesized as reported in the literature.[3,57] The molybdenum complexes **11** were prepared by a thermal reaction of **9** with Mo(CO)$_6$ in refluxing *n*-heptane (Scheme 3), conditions previously shown to be suitable for the reactions of **7** (Scheme 1).[53] Over the course of 4–8 h, the solution IR bands of aliquots taken from the reaction mixture slowly lost bands from Mo(CO)$_6$ and were replaced by a new pattern diagnostic of LMo(CO)$_5$. The reaction was stopped when the hexacarbonyl peak no longer decreased; meanwhile the solution turned from colourless to bright yellow-green. Direct cooling of these yellow solutions produced a reasonable yield of crystalline solids that could be recrystallized from the same solvent to afford analytically pure materials that were also suitable for crystallography. Similar direct thermal reactions of Cr(CO)$_6$ and W(CO)$_6$ do not go to completion and on prolonged heating lead to decomposition rather than the desired products. LM(CO)$_5$ complexes **10** and **12** were instead obtained by a reaction with photochemically produced (THF)-M(CO)$_5$ at room temperature in THF as the solvent.[58] The ligands readily displace THF to form the products. After the reaction was judged complete based on solution FTIR aliquots,

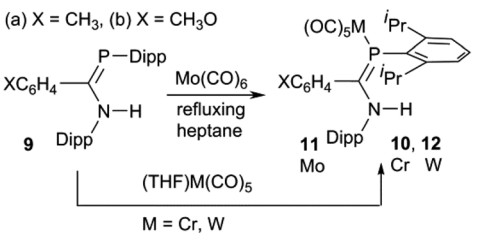

Scheme 3

the THF was removed and the products recrystallized from THF or diethyl ether.

Crystal structures

The compositions of the ligands **9** and their $M(CO)_5$ complexes **10–12** have been confirmed by using single-crystal X-ray structures, all determined on an area-detector diffractometer at RT. The structure of **9a** was previously published.[3] The molecular structure with the atom numbering scheme of **9b** is presented in Fig. 1. As the Cr, Mo and W complexes of **9a** are isostructural, only the molecular structure of **10** is presented in Fig. 2 with the common atom numbering scheme (for **11a** and **12**, see Fig. S1 and S2 in the ESI†). The major component of the disorder model for the molecular structure of **11b** is presented in Fig. 3. Selected interatomic distances and angles are shown in Table 1 whilst the crystal and parameter data are found in Table S3.† None of the structures have significant intermolecular contacts and in particular neither the ligands nor the metal complex display conventional hydrogen bonding involving the NH group.

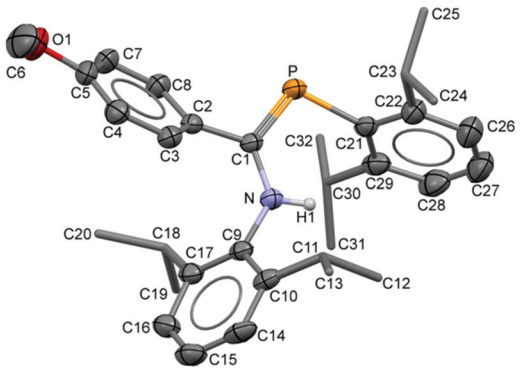

Fig. 1 Displacement ellipsoid plot (30% probability) of the molecular structure of **9b** as found in the crystal structure (295 K). The atom numbering scheme is provided; H atoms on C are omitted and the ^{i}Pr C are rendered as tubes for clarity.

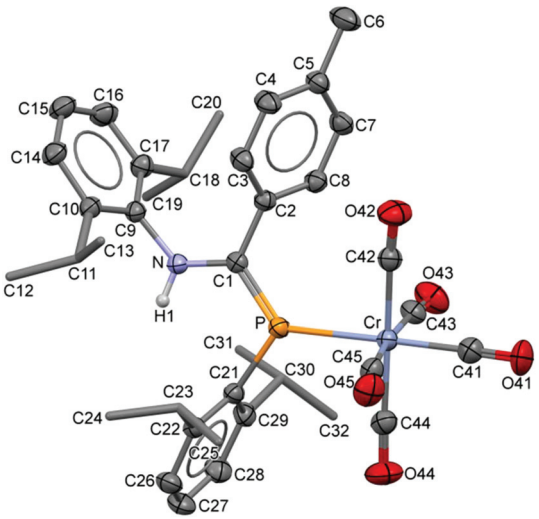

Fig. 2 Displacement ellipsoid plot (30% probability) of the molecular structure of **10** as found in the crystal structure (295 K). The atom numbering scheme is provided; H atoms on C are omitted and the ^{i}Pr C are rendered as tubes for clarity. The isostructural Mo and W complexes use the same numbering scheme (Fig. S1 and S2†).

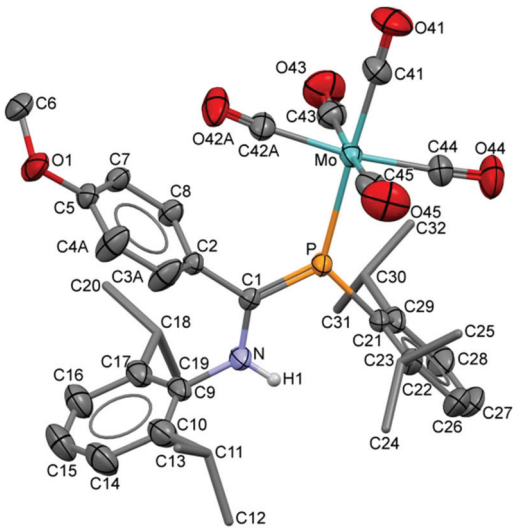

Fig. 3 Displacement ellipsoid plot (30% probability) of **11b** as found in the crystal (295 K). Atom numbering schemes are shown; H atoms on C are omitted and the ^{i}Pr C are rendered as tubes for clarity. Disorder in the C42/O42 carbonyl groups and in C3/C4 refines with a two-part model; the major (65%) component is shown.

All four metal complexes share the same gross features: the ligand is connected *via* the *n*(P) HOMO−1 orbital (see below) in the common κ*P* coordination mode.[13,18] In each case, the phosphaamidine backbone composed of C1, C2, P, N, C9 and C21 is found to be planar and M lies in or close to this plane (defined as "plane 1", see Table 1). All three aryl rings (planes 2–4 in Table 1) approach a perpendicular orientation (∠60°–∠88°) to this plane; the rotation of the backbone tolyl or mesityl rings, ∠Pl1–Pl2, is 15–20° larger than in **9**. In all cases, the solid state structures contain the ligands in the *Z-anti*-(P═C) *C*-amino-(λ^3,σ^2)-aminophosphaalkene geometry (as is also found in the crystal structures of **9**) with the $M(CO)_5$ groups in the *exo* position. In these conformations, the ^{i}Pr groups of the phosphino Dipp rings provide "side shields" for the phosphorus nucleus as well as the P═C π bond. Within the molecular structures, **11b** has a planar phosphino Dipp ring from which the P atom deviates by only 0.0693(4) Å. The isostructural series **10**, **11a** and **12** have deviations of 0.29–0.30 Å. Consideration of Table 1 also confirms that the metric parameters of the coordinated phosphaamidines **10–12** are very similar to those of the free molecules **9**. The average P═C bond length among all four metal complexes is 1.702(3) Å and the N–C bond length is 1.359(7) Å (errors here are std. dev.), statistically indistinguishable from the values in **9**. In **11a** the P–C1–C2 angle has opened up to 118.80(15)° compared to 116.4(2)° in **9a**, whilst the sums of angles around C1

Table 1 Selected interatomic distances (Å) and angles (°) from the crystal structures and DFT calculations[a]

Parameter	9a[a]	9b	10	10 (DFT)[b]	11a	11b	12
P–C1	1.709(2)	1.716(2)	1.701(2)	1.771	1.7031(19)	1.697(2)	1.706(5)
N–C1	1.367(3)	1.365(3)	1.361(3)	1.372	1.365(3)	1.362(4)	1.346(8)
C1–C2	1.488(3)	1.480(3)	1.484(3)	1.486	1.488(3)	1.485(3)	1.477(8)
P–C21	1.847(2)	1.849(2)	1.834(2)	1.896	1.839(2)	1.837(3)	1.834(6)
N–C9	1.430(3)	1.434(3)	1.447(3)	1.452	1.442(2)	1.446(3)	1.441(7)
N–H1	0.860	0.87(2)	0.86(3)	1.018	0.83(2)	0.856(18)	0.88(2)
P–M	—	—	2.4259(7)	2.507	2.5612(6)	2.5559(8)	2.5378(16)
M–C41	—	—	1.845(3)	1.824	1.984(3)	1.967(4)	1.982(7)
M–C42	—	—	1.905(3)	1.872	2.059(3)	2.056(9)	2.034(7)
M–C43	—	—	1.905(3)	1.871	2.064(3)	2.033(4)	2.063(8)
M–C44	—	—	1.884(3)	1.866	2.036(3)	2.016(3)	2.015(7)
M–C45	—	—	1.881(3)	1.867	2.025(3)	2.028(4)	2.036(7)
C41–O41	—	—	1.143(3)	1.183	1.141(3)	1.144(4)	1.141(9)
C42–O42	—	—	1.133(3)	1.177	1.130(3)	1.134(9)	1.144(9)
C43–O43	—	—	1.135(3)	1.178	1.127(3)	1.140(4)	1.121(10)
C44–O44	—	—	1.138(3)	1.179	1.128(3)	1.137(4)	1.145(9)
C45–O45	—	—	1.145(3)	1.179	1.147(3)	1.143(4)	1.138(9)
P–C1–N	123.4(2)	123.11(18)	122.98(16)	123.7	123.28(15)	124.53(19)	123.3(4)
P–C1–C2	116.4(2)	115.80(18)	119.41(16)	117.8	118.80(15)	118.33(18)	118.8(4)
N–C1–C2	120.0(2)	120.9(2)	117.61(17)	118.4	117.92(17)	117.1(2)	117.9(5)
C1–N–C9	131.7(2)	130.9(2)	125.0(2)	126.5	125.2(5)	124.8(2)	125.9(5)
C1–P–C21	101.9(1)	103.54(11)	106.73(10)	105.1	107.11(9)	106.23(12)	107.1(3)
C1–P–M	—	—	130.38(8)	127.4	130.41(7)	130.05(9)	130.3(2)
C21–P–M	—	—	121.09(6)	124.8	121.25(6)	123.66(8)	121.09(18)
C1–P–C21	101.9(1)	103.54(11)	106.73(10)	105.1	107.11(9)	106.23(12)	107.1(3)
C1–N–H	—	—	113.7(16)	116.1	115.5(16)	116(2)	124(5)
C1–N–C9	—	—	125.02(18)	126.5	125.25(17)	124.8(2)	125.9(5)
P–M–C41	—	—	177.63(9)	175.8	177.48(8)	177.13(12)	177.3(2)
P–M–C42	—	—	91.81(7)	96.1	92.16(7)	98.0(3)	91.8(2)
P–M–C43	—	—	90.99(8)	87.1	91.53(7)	91.78(10)	91.0(2)
P–M–C44	—	—	88.90(8)	88.3	88.86(8)	88.54(10)	88.6(2)
P–M–C45	—	—	95.58(8)	90.6	95.72(7)	93.37(10)	96.2(2)
C1–P–M–C42			26.1(1)	7.9	23.6(1)	4.1(3)[f]	24.9(3)
∠Pl1–Pl2[c]	42.57	45.17(6)	61.89(09)	59.8	60.36(8)	74.3(2)	60.8(2)
∠Pl1–Pl3[d]	59.55	57.88(8)	75.83(8)	83.6	75.56(7)	79.3(1)	75.5(2)
∠Pl1–Pl4[e]	77.66	61.9(1)	79.66(9)	84.0	83.41(8)	88.2(1)	84.0(2)

[a] Ref. 3. [b] Geometry optimized B3PW91/LANL2DZ hybrid DFT calculations, confirmed to have zero imaginary frequencies (Fig. S4). [c] Plane 1: C21, P,C1,N,C9; plane 2: C2,C3,C4,C5,C7,C8. [d] Plane 3: C9,C10,C14,C15,C16,C17. [e] Plane 4: C21,C22,C26,C27,C28,C29. [f] C1–P–Mo–C42A; for C1–P–Mo–C42B, 18.9(5)°.

remain very close to 360°: 359.9(3)° and 360.0 (3)°, respectively. It is the N–C1–C2 angle that closes to make up the difference, perhaps indicative of steric crowding of the tolyl ring by the equatorial CO groups of the metal. The same effect is observed for the structures of **10**, **11a** and **12**.

There has been extensive discussion in the literature on the structural consequences of amine substitution on phosphaalkenes, which can have a dramatic effect on geometry. In order to fit **10–12** into a suitable context, a survey was undertaken of all non-cyclic phosphaalkene complexes of Group 6 $M(CO)_5$ reported in the Cambridge Structural Database (CSD). The results are compiled in Table S1† along with the CSD refcodes and literature citations (for readers without access to the CSD, diagrams of all cited structures are provided in Fig. S3†). There is in fact wide diversity amongst these structures and there are relatively few "conventional" phosphaalkenes where the C is substituted only with hydrocarbon groups, so that to make sense of the data the types of substituents $R^{1,2}$ at C and R at P are also listed along with a descriptive phrase of the compound type. The results have been compiled into a histogram shown in Fig. 4.

Within this histogram there are two distinct regions, the majority of exemplars centred on 1.67 Å (labelled "A"–"C" in Fig. 4) which are structurally uniform and display "end-on" coordination from the in-plane *n*(P) orbital, despite the wide diversity of substituents. There is also an outlying group "D" nearer 1.80 Å, which are molecules with one or two dimethylamino groups at the P=C carbon, and are all coordinated "side-on" to the metal, albeit through the P atom only.[47–49] Within the major distribution, it is possible to distinguish two distinct groups: group "A", ranging from *d*(P=C) 1.61 Å–1.68 Å, which can be attributed to phosphaalkenes bearing only H or organic moieties (including cumulenes) at carbon; and Group "C", extending from 1.67 Å to 1.71 Å, which are phosphaalkenes where one of the substituents at C is an alkoxy group (so-called Becker phosphaalkenes),[60] or are very strained organic groups such as cyclopropane. This group includes **10–12**. The overall distribution maximum "B" at

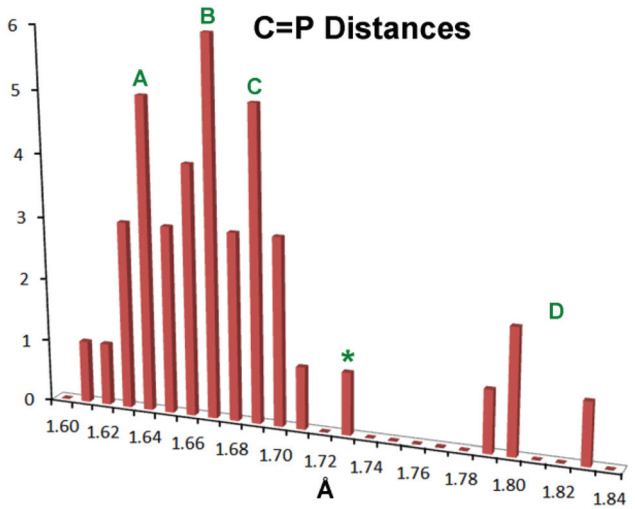

Fig. 4 Histogram showing P═C bond distances in known metal Group 6 $M(CO)_5$ complexes of acyclic phosphaalkenes and related complexes (CSD Release 5.36, May 2015).[59] See the text for details.

1.67 Å borrows intensity from these neighbouring distributions. Thus, substitution at the P═C carbon by a single aromatic amine such as the DippN groups does not lead to distinctly longer P═C bonds, although **10–12** certainly flank the long-end slope of the distribution.

So what is going on with the outlier aminophosphaalkenes in Table S1† and Fig. 4? The peak marked * belongs to **13** (Chart 2; refcode ENEBUU).[46] The structures in group "D" are, in order of increasing *d*(P═C), **14** (GEJYUP),[49] **15** (VOJMUC)[48] and **16** (CODNUE).[49] All of these have one or two NMe_2 substituents at C and most also have strongly electron-withdrawing groups on P (**14–16**). It is instructive to compare these with **10–12** using two additional criteria: (i) the deviation of P out-of-plane (oop) of its attachment points (M, C1 and C21 in our numbering scheme); (ii) the dihedral angle between the planes defined by M, P plus the three carbonyl C atoms within the M,P plane (C41, C42 and C44 in our numbering scheme) and the plane containing the P═C bond (P, N, C1, C2, C21 and C9 in our numbering scheme). The P oop distances (Å) are: **11b**, 0.03; **10**, 0.15; **11a**, 0.13; **12**, 0.14; **13**, 0.38; **14**, 0.87 and 0.90; **15**, 0.82; **16**, 0.61 (listed in the order of P═C distances in Table S1†). The specified dihedral angles (°) are: **11b**, 12.2; **10**, 15.3; **11a**, 14.7; **12**, 14.7; **13**, 42.3; **14**, 64 and 64.0; **15**, 62.6; **16**, 49.8. Both series correlate strongly with *d*(P═C) (R^2 = 0.85 and 0.84, respectively, see Fig. S5†). Evidently, strong hybridization towards pyramidal phosphorus is associated with $M(CO)_5$-coordinated phosphaalkenes bearing very strong electronic donors at C, especially when accompanied by electron withdrawing groups at P. This re-hybridization has the consequence of greatly lengthening the P–C bond. Such distortions do not occur in **10–12** which fit in sequence with other κ*P*-coordinated phosphaalkenes.

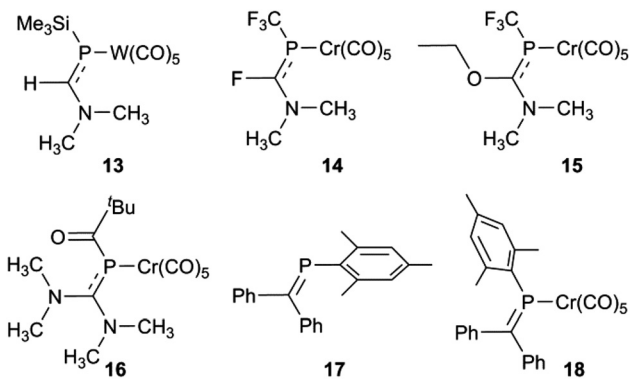

Chart 2

Solution structure: NMR evidence

The ^{1}H NMR data for, in particular, the ^{i}Pr methyl groups are diagnostic of the solution-phase behaviour of phosphaamidines **9** and complexes **10–12**. These data are compiled in Table 2 along with those for the methine signals; 2-D NMR has been used to confirm the assignments, starting from the methine signals for the Dipp group attached to phosphorus, which are unambiguously identifiable as doublets of septets from coupling to ^{31}P (*f* in Fig. 5). From this it can be easily established that the signals labelled as **A** and **B** are for methyl groups attached to the amino Dipp ring. Scheme 4 shows the relative orientation for the three most likely isomeric forms for **9a** in its phosphaalkene isomer. In the *Z-anti*(P═C) conformation alone, methyl groups on this ring experience significant anisotropic ring-shielding from the (the more proximate) backbone aryl group at **A** and from the (somewhat more distant) phosphine Dipp ring at **B**. These effects induce the unusual high-frequency chemical shifts for methyls **A** and **B**. By contrast, the methyl groups of the phosphino Dipp ring are at normal chemical shifts; the differentiation whereby **C** is mildly shifted to higher frequency can possibly be attributed to a weak anisotropic shielding from the P═C π system. Note with reference to Scheme 4 that neither the *E-anti* nor *E-syn* geometries are able to induce such a pattern of anisotropic shielding distributed to these specific methyl groups. *E-anti* would affect one methyl group on each of the Dipp rings, whereas *E-syn* is expected to have the anisotropic shielding effect on the phosphino Dipp ring.

An interesting feature of the spectra of the complexes is that the high-frequency methyl signals **A** and **B** are somewhat line-broadened compared to **C** and **D** (an effect absent in free **9**). This implies somewhat slow rotation of the ^{i}Pr groups on the amino Dipp ring, consistent with stronger steric congestion with the backbone aryl group (the smaller C–N–C angle in the complexes has already been noted). Table 2 also reports the NMR data for the major isomers observed for **9** in $CDCl_3$ (the isomer distributions are strongly solvent-dependent). The remarkable similarity of the data between **9a** and complexes **10**, **11a** and **12** as well as between **9b** and **11b** provides strong evidence that the geometry of this majority solution-phase

Table 2 ^{1}H and ^{31}P NMR data for non-aromatic nuclei in phosphaamidines and carbonyl complexes[a]

Atom/Grp	Parameter	9a[b]	9b[b]	10	11a	11b	12
^{i}Pr–CH$_3$ **A** (amino)	δ (^{1}H)	0.81	0.83	0.86[c]	0.79[c]	0.88[c]	0.88[c]
	$^{3}J_{HH}$, Hz	6.7	6.9	6.6	6.7	6.7	6.7
^{i}Pr–CH$_3$ **B** (amino)	δ (^{1}H)	0.89	0.92	0.99[c]	0.92[c]	0.98[c]	0.97[c]
	$^{3}J_{HH}$, Hz	6.7	6.9	6.7	6.7	6.9	6.7
^{i}Pr–CH$_3$ **C** (phosphino)	δ (^{1}H)	1.27	1.27	1.36	1.29	1.35	1.36
	$^{3}J_{HH}$, Hz	6.9	6.7	6.7	6.7	6.7	6.7
^{i}Pr–CH$_3$ **D** (phosphino)	δ (^{1}H)	1.35	1.36	1.47	1.40	1.45	1.47
	$^{3}J_{HH}$, Hz	6.9	6.9	6.7	6.7	6.7	6.7
R = 4-CH$_3$ *or* 4-CH$_3$O	δ (^{1}H)	2.22	3.70	2.22	2.15	3.71	2.23
	$^{7}J_{PH}$, Hz	—	—	1.8	1.8	—	1.8
^{i}Pr–H (amino)	δ (^{1}H)	3.00	3.00	2.96	2.96	3.01	3.02
	$^{3}J_{HH}$, Hz	6.7	6.8	6.7	6.6	6.6	6.8
^{i}Pr–H (phosphino)	δ (^{1}H)	3.84	3.85	4.00	3.91	4.00	3.99
	$^{3}J_{HH}$, Hz	6.9	6.7	6.7	6.7	6.7	6.7
	$^{4}J_{PH}$, Hz	3.4	3.4	4.6	4.6	4.7	4.6
N–H	δ (^{1}H)	6.24	6.24	6.50*	6.43*	6.45*	6.45*
	$^{3}J_{PH}$, Hz	1.0	2.4	—	—	—	—
^{31}P NMR	δ (^{31}P)	53.6	51.4	45.0	30.2	29.6	6.0
	$^{1}J_{WP}$, Hz						255
	$\Delta\delta$(^{31}P)			−8.4	−23.2	−21.8	−47.4

[a] NMR data recorded in $CDCl_3$. [b] The major one amongst four solution species. [c] Somewhat line broadened.

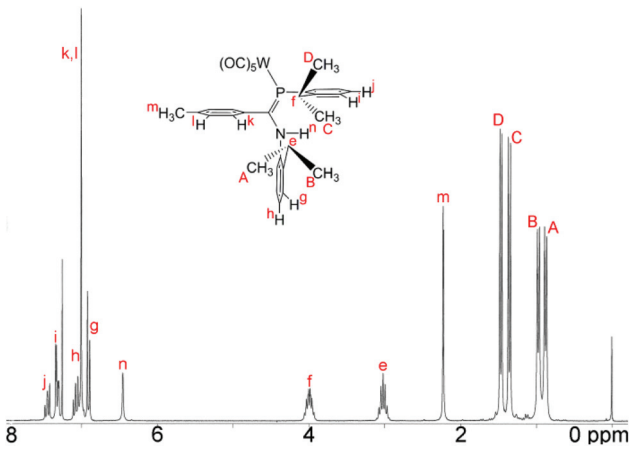

Fig. 5 ^{1}H NMR spectrum ($CDCl_3$) of the tungsten carbonyl complex **12**. Labels indicate the assignment.

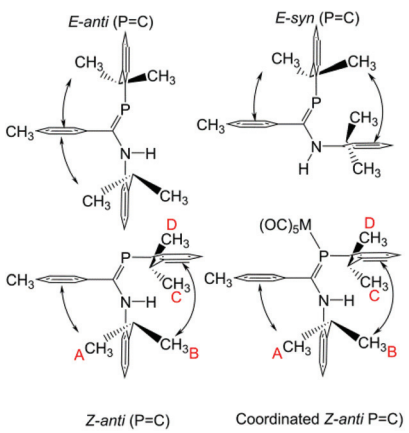

Scheme 4 Accessible solution-phase geometries.

isomer is also *Z-anti*(P=C), as also occurs in their crystal structures (ref. 3 and Fig. 1).

The ^{31}P chemical shifts of the complexes are all at higher frequencies compared to **9**, with the magnitude of $\Delta\delta$(^{31}P) increasing in the order Cr < Mo < W. A similar trend has been reported for other λ^3,σ^2 compounds[61] and is also well-known for triorganophosphine LM(CO)$_5$ complexes.[62] In **12** the value of ^{1}J(^{183}W–^{31}P) = 255 Hz. Mathey and co-workers prepared a number of reactive Ph–P=CR$_2$ as the W(CO)$_5$ complexes, which have $^{1}J_{WP}$ ranging from 251 to 259 Hz; for similar ^{t}Bu–P=CR$_2$ the values are 244–245 Hz. Yoshifuji *et al.* reported for a series of W(CO)$_5$ complexes of Mes*–P=CR$_2$ that $^{1}J_{WP}$ ranges from 269 to 273 Hz. The "Becker" phosphaalkene (Me$_3$Si)$_2$CH–P=C(Ph)OC(=O)Ph W(CO)$_5$ complex is reported to have $^{1}J_{WP}$ = 267 Hz.[41] This small sampling suggests that only substituents on phosphorus have a distinct influence on the size of the one-bond metal–phosphorus coupling; indeed it has been demonstrated that the size of $^{1}J_{WP}$ in LM(CO)$_5$ complexes depends primarily on the electronegativity of the substituents directly attached to phosphorus.[62,63] The only other amino-substituted compound available for comparison is Me$_3$Si–P=C(H)–NMe$_2$ for which $^{1}J_{WP}$ = 186 Hz;[46] since the trimethylsilyl group is so much more electropositive than a Dipp group, no meaningful conclusion can be drawn from this comparison.

Only limited ^{13}C data were obtained, since **10** is the only complex to resist decomposition long enough for the accumulation of a good spectrum. The ^{13}CO data for **10** (δ(CO$_{eq}$) 216.0, $^{2}J_{PC}$ = 15.1 Hz; δ(CO$_{ax}$) 229.9, $^{2}J_{PC}$ = 4.9 Hz) are very similar to those in **18** (δ(CO$_{eq}$) 214.8, $^{2}J_{PC}$ = 16 Hz; (δ(CO$_{ax}$) 221.4, $^{2}J_{PC}$ = 3 Hz). All these resonances are deshielded compared to Cr(CO)$_6$, δ(CO) = −211.2,[64] but the greater deshielding of the axial ^{13}CO indicates lower π acceptor and higher σ donor ability of the

trans ligand compared to carbon monoxide.[65] By this criterion, a $\Delta\delta$ from the hexacarbonyl shift, there is little difference in the π_{acc}/σ_{don} ratios between **10**, $\Delta\delta$ = 6.9, and **18**, $\Delta\delta$ = 6.6 ppm.

Infrared spectra

The infrared spectra in the ν(NH) and ν(C≡O) regions for **9–12** are presented in Table 3. It is well-known that the $A_1(2)$ vibration in $LM(CO)_5$ complexes reflects the stretching frequency of the axial CO group that is *trans* to L.[66] This mode should have considerable intensity, though generally it is found to be less intense than E. It is also the case that the E mode can split under conditions of lowered symmetry, either due to a very asymmetrical ligand L or due to symmetry lowering from lattice effects. Unlike many of the classic ligands in coordination chemistry including R_3P, the data for $LM(CO)_5$ phosphaalkenes are rather scattered and incomplete. We have therefore taken great care to collect data in several solvents – for ease of comparison with the literature data – and at various concentrations. We consider the data collected in *n*-heptane to be the most similar to gas-phase values, and assign the weak band at around 2070 cm^{-1} to $A_1(1)$, a non-controversial assignment. The B_2 band is always extremely weak. For the remaining carbonyl stretching bands, based on the variability of the low-energy bands to conditions and literature precedents, we tentatively assign those at ~1950 cm^{-1} to the $A_1(2)$ vibration, and the remaining bands to a split in the E band induced by the large, asymmetric ligands. In chloroform solution, the E vibration is found to be even more intense and is sufficiently broad to overlap the $A_1(2)$ vibration almost completely. The bands at ~1930 cm^{-1} (heptane), ~1915 cm^{-1} ($CHCl_3$) and ~1907 cm^{-1} (KBr) are assigned to the other branch of the E vibration. These assignments are confirmed by the results of the B3PW91/LANL2DZ frequency calculation on the optimized geometry of **10** (Table 3 and Fig. 6).

There are very few solution-phase IR data available for the many $M(CO)_5$ complexes in the literature; most reports are from solids in KBr or from Nujol™ mulls, data that are more susceptible to lattice effects. The spectrum of the $Cr(CO)_5$ complex **18** of phosphaalkene **17** was reported in cyclohexane with ν(C≡O) of 1955 and 1901 cm^{-1}, with the former taken as $A_1(2)$.[31] More complete data are available for the $Cr(CO)_5$ complex of $Cp^*(CO)_2Fe$–C(H)=P–$CH(SiCH_3)_2$ which has a short P=C bond similar to conventional phosphaalkenes (refcode TACKOX in Table S1†): cyclopentane solution, 2067(m), 1980(w), 1945(vs), 1935(vs), 1931(vs) cm^{-1}.[28] These data are almost indistinguishable from those of **10** in *n*-heptane. The $Cr(CO)_5$ complex of κ*P*-2,4,6-triphenylphosphorine by contrast has an $A_1(2)$ vibration at 1968 cm^{-1}, indicative of a higher π_{acc}/σ_{don} ratio.[67] Furthermore, the $A_1(2)$ data for **10–12** are very close to those of $M(CO)_5$ complexes of R_3P (at Cr, R = Ph: 1944 cm^{-1}; R = ^{t}Bu: 1937 cm^{-1}).[67] Taken together, these data suggest that **9** are weak π-acceptors and good σ-donors and not significantly different, in this regard, from conventional phosphaalkenes.

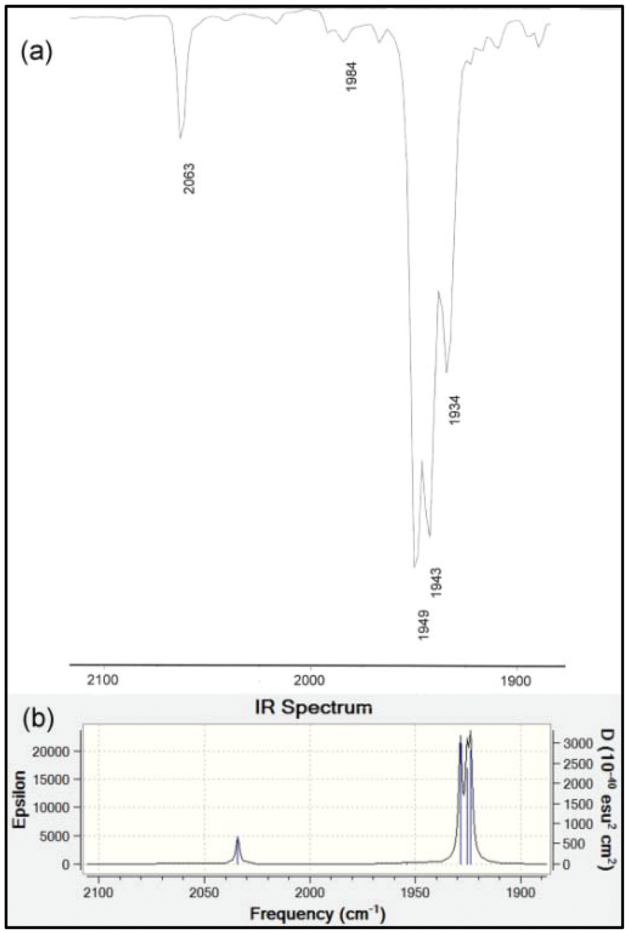

Fig. 6 (a) Experimental solution IR spectrum in the carbonyl stretching region of **10** measured dilute in hexane. (b) Computed gas-phase IR spectrum at the B3PW91/LANDL2DZ level of theory (data in Table 3).

Table 3 Infrared spectra of phosphaamidines and metal complexes[a]

n-Heptane	NH	CO $A_1(1)$	CO B_2	CO $A_1(2)$	CO E_a	CO E_b
9a	3354 m					
9b	3354 m					
10	—	2063 w	1984 w	1949 vs	1943 vs	1934 s
10 (DFT calc.)[b]	3561 w	2034 m	1954 w	1929 vs	1926 s	1924 vs
11a	—	2072 w	1989 w	1955 vs	1947 vs	1933 s
11b	—	2071 w	1989 w	1955 vs	1947 vs	1933 s
12	—	2070 w	1989 w	1948 vs	1939 vs	1929 s

[a] FTIR data in solution (cm^{-1}); for additional solvent and KBr pressed-pellets, see Table S2. [b] From a frequency calculation on the optimized geometry using B3PW91/LANL2DZ, uncorrected.

Bonding in metal complexes

Surprisingly little investigation has been undertaken on the electronic structures of $M(CO)_5$ complexes of phosphaalkenes despite the many examples of such compounds that have been prepared over the past forty years. An early observation of facile *E*/*Z* isomerism of a coordinated conventional phosphaalkene[68] elicited an investigation using EHMO methods.[69]

These authors concluded that phosphaalkenes coordinate to $Cr(CO)_5$ *via* σ bonds and that any π bonding is negligible. This conclusion is in error at least insofar as they predicted that the C1–P–M–C42 dihedral angle minimizes to 45° and that rotation of the P–M bond is facile. A consideration of all the structures in the main distribution in Fig. 6 consistently shows that this dihedral is close to zero. In the crystal structures of **10–12**, this dihedral (Table 1) ranges from 8.3(2)° to 26.1(1)°; in the B3PW91/LANL2DZ optimized geometry it is only 7.9°. This suggests that the phosphaamidine geometry adopts an eclipsed orientation to the metal CO ligands against the opposing steric forces.

More recently, DFT calculations using modified SBK effective core potential basis sets were reported in which two model ligands, namely $HP{=}CH_2$ and $HP{=}C(H){-}NH_2$, are coordinated to $M(CO)_5$ (M = Cr, Mo, W).[51] This paper seems primarily devoted to explaining the highly-distorted coordination mode exhibited in **14** and **15**, including the discovery that complex **14** is capable of attaching to a second $Cr(CO)_5$ group at P.[70] These studies demonstrate that such bis metal coordination is likely induced by the strongly electron-withdrawing CF_3 groups at P. The calculations also show that the geometry of the model phosphaalkene and aminophosphaalkene do not change much in the singly-coordinated, κ*P* mode. This report is scarce in other details of the calculations and does not address the electronic structures of these complexes in detail. We have therefore undertaken DFT studies using the B3PW91 functional on the full molecular structure of **10** (Fig. 7b), a method which has previously shown good results in our hands for low-valent chromium complexes. In this study, the effective core potential basis set LANL2DZ was employed which has been shown to give good results for early transition metals. To gain further perspective, a similar set of calculations was performed on **18** (Fig. 7a), one of the best-known conventional phosphaalkene $Cr(CO)_5$ complexes. The computed geometry of **10** included in Table 1 is in good agreement with the experimentally-determined results (see also Fig. S4† for pictures of the structure and an overlay with the X-ray geometry). A fragment orbital analysis was then developed using the LANL2DZ results (on the X-ray geometries) in conjunction with PM3 semi-empirical calculations for the fragments (Fig. 7c).

The frontier molecular orbitals (FMO) of the $Cr(CO)_5$ fragment in the centre of the diagram are well known, consisting of an empty Cr d_{z^2} orbital and three filled d_{xz}, d_{yz} and d_{xz} orbitals (in this orientation, $d_{x^2-y^2}$ is bonding to the equatorial carbonyl ligands).[69] The FMOs of $Mes{-}P{=}CPh_2$, **17**, are shown on the right, consisting of the π(2) LUMO, the π(1) HOMO and just below this the *n*(P) orbital. This is in full agreement with the earlier DFT study except that Fig. 7c also shows the filled aromatic π orbitals from the Mes and Ph rings that are not present in the simple model ligands.[51] The interaction of these fragments to form **18** is dominated by σ-bonding between the metal LUMO (d_{z^2}) and the HOMO−1 of the phosphaalkene. The bonding interaction stabilizes well below the filled aromatic π orbitals (shown as boxes in the diagram). Metal d_{xz} and d_{yz} orbitals are non-interacting with the incoming

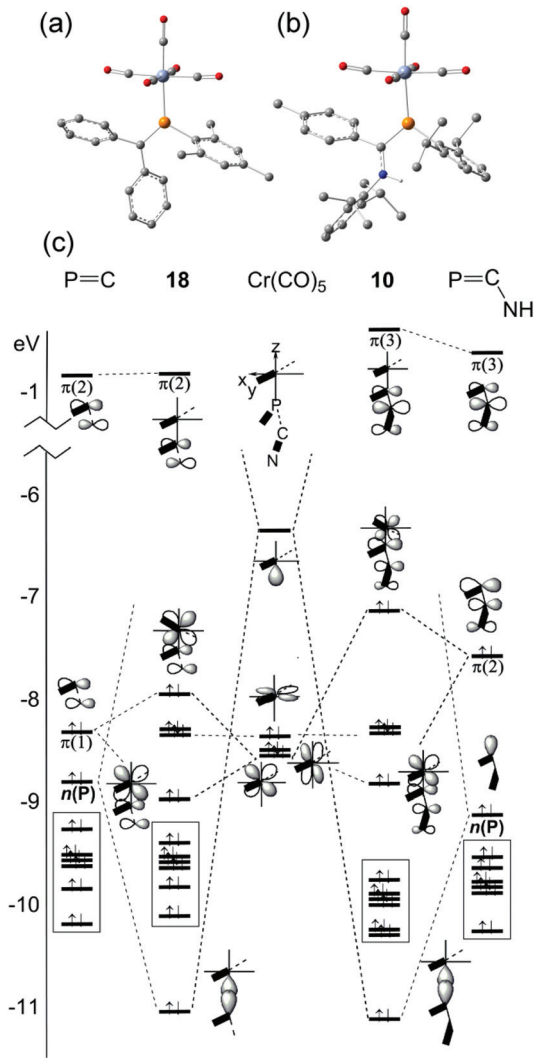

Fig. 7 Geometry-optimized B3PW91/LANL2DZ computed electronic structures of (a) **18** and (b) **10**. (c) Comparative orbital interaction diagrams for **18** and **10**, showing energy levels and orbital topologies confirmed by B3PW91/LANL2DZ calculations using the X-ray structure geometries with the un-optimized ligand and $Cr(CO)_5$ fragments.

ligand; the net π interaction is between the metal d_{xz} and ligand π(1) orbitals, resulting in two new filled π-type orbitals. The net effect raises the HOMO energy in the complex (for which, see below). These calculations also confirm that there is very little interaction with the high-lying π(2) MO which transforms almost unchanged into the complex and remains the LUMO. The "net π bonding/antibonding" in **18** therefore depends on the relative strengths of the interactions in the HOMO and HOMO−3 of the complex.

The FMOs of the aminophosphaalkene isomer of **9a** are shown on the far right of the diagram. These differ from **17** by the presence of the strongly donating nitrogen p_x orbital (not shown), resulting in a new π(1) that has strong C=N π bonding character.[51] As a consequence, the HOMO is now π(2) and is raised considerably in energy compared to the HOMO

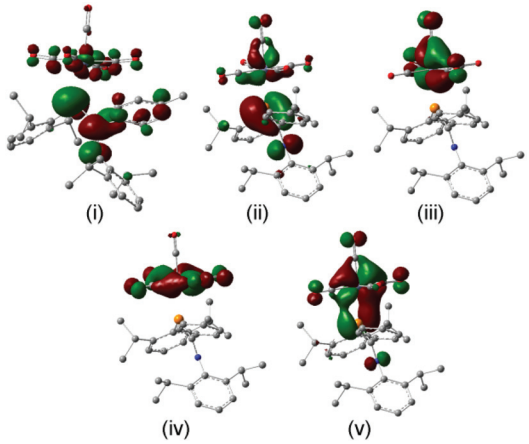

Fig. 8 Frontier molecular orbitals from the geometry-optimized B3PW91/LANL2DZ calculations on **10**: (i) the LUMO with predominantly ligand π(3) character; (ii) the HOMO with ligand π(2) antibonding to d_{yz}; non-interacting (iii) d_{xz} and (iv) d_{xy} MOs; (v) the bonding ligand π(2)–d_{yz} combination.

of **17**. The electronegativity of the nitrogen also serves to lower the energy of HOMO−1 which still has predominantly *n*(P) character and still forms the dominant bonding interaction with the metal LUMO, which again stabilizes below the filled aromatic π ligands (boxed). The bonding (HOMO−3) and antibonding (HOMO) interactions again determine the net π-bonding character. Unlike in **18**, in **10** the π(3) LUMO is weakly destabilized. The key FMOs in **10** are shown more accurately in Fig. 8 than in the cartoons within Fig. 7c. These pictures help to emphasize: (i) the out-of-phase interaction between π(3) and the d orbitals in the LUMO; (ii) the destabilizing d–p π interaction in the HOMO that is evidently dominated by the ligand in **10** and the non-interacting HOMO−1 and HOMO−2 dominated by metal d_{yz} and d_{xy} in (iii) and (iv). Finally, in (v) the in-phase d–p π interaction has more metal than ligand character in **10** than is the case for the equivalent orbital in **18**. This difference in the characters of HOMO and HOMO−3 is a direct consequence of the higher-lying ligand π HOMO in **9** compared to **17**. These calculations also corroborate the spectroscopic evidence that there is no obvious π-backbonding in either **10** or **18**. The π interactions more or less cancel out each other for these zero-valent complexes with these electron-rich ligands. The bonding is therefore predominantly, but not exclusively, of σ character.

Electronic spectra

Having developed a pictorial representation for the orbital manifolds in **10** and **18**, it is now fruitful to consider the electronic absorption spectra. The data for the complexes are shown in Table 4, and representative spectra obtained in hexanes solution are provided in Fig. 9. The colours of the ligands **9** and the metal complexes **10–12** are all yellow. The ligands have a low-energy, rather intense, absorption in the visible responsible for their yellow colours with maxima around 28 000 cm^{-1} which can be confidently assigned to allowed $\pi^* \leftarrow \pi$ transitions.

For each of the metal complexes, there is a distinct bathochromic shift in λ_1, while retaining considerable intensity ($\log \varepsilon \approx 4$), which we therefore also ascribe to an allowed $\pi^* \leftarrow \pi$ transition. More detailed assignments will require sophisticated calculations that are beyond the scope of this paper. Qualitatively, the data show that in **10–12**, the HOMO–LUMO gap is lowered by some 3400 to 3500 cm^{-1} in the complexes compared to the free phosphaamidines, which amounts to 13% reduction in the energy gap. By contrast, in the conventional phosphaalkene **17**, complexation to $Cr(CO)_5$ lowers the HOMO–LUMO gap by some 6000 cm^{-1}, a reduction in the energy gap of 20%.[31] These data can be understood in the context of the changes in energy levels shown in Fig. 7c. Whilst the HOMO of **18** is considerably increased in energy due to the repulsive π interaction with the ligand, the LUMO is predicted to remain unchanged, and hence ΔE is significantly reduced in the complex. In the case of **10**, while the HOMO is also increased in energy, so is the LUMO and hence ΔE is reduced by a smaller amount. Finally, it is worth mentioning that the typical yellow colours of phosphine-substituted LM$(CO)_5$ complexes of Group 6 metals are usually attributed to an MLCT process.[58] Insofar as the HOMOs of both **10** and **18** are calculated to have more metal d character than their LUMOs, this generalization is also valid for phosphaalkene and phosphaamidine complexes.

Table 4 Electronic absorption spectra of amino- and conventional phosphaalkenes[a]

Compound	λ_1	λ_2	λ_3	λ_4
9a	28 000 (4.15)	36 000 (4.04)	43 300 (4.30)	>50 000[c]
10	24 500 (3.93)	~34 000 sh {~4.1}	40 800 (4.46)	48 300 (4.85)
11b	25 300 (4.01)	35 700 sh (~4.14)	40 500 (4.51)	>47 600
12	24 600 (3.98)	35 700 (4.08)	41 800 (4.56)	41 800 (4.56)
17[b]	30 900 (2.84)	37 300 (3.01)	39 400 (4.20)	—
18[b]	24 900 (4.28)	—	39 500 (4.73)	—

[a] Measured in hexanes in 10 mm quartz cuvettes. Data in cm^{-1} with $\log \varepsilon$ in parentheses. [b] Ref. 31 – both measured in THF. [c] 49 300 (4.87) in CH_3OH solution.

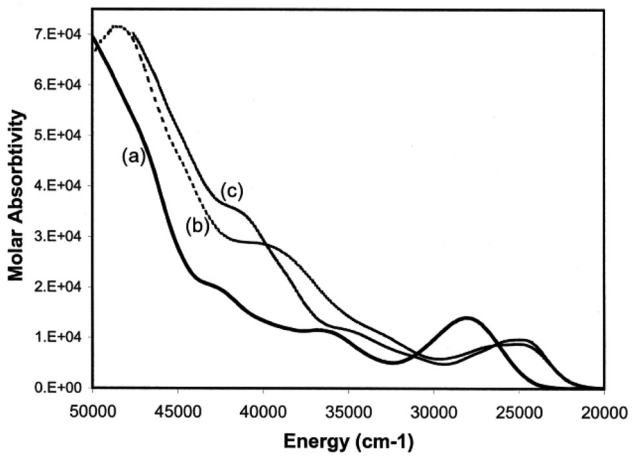

Fig. 9 Electronic absorption spectra of (a) **9a**, (b) **10** and (c) **12** in hexane solutions.

Conclusions

Replacement of one nitrogen atom in bulky aryl *N*,*N*′-disubstituted amidines by phosphorus produces the atom-equivalent *N*,*P*-monophosphaamidines. This element-exchange has a profound effect on the coordination of these ligands as neutral molecules in $LM(CO)_5$ complexes of Cr, Mo and W. Whereas the all-nitrogen bulky amidines can coordinate weakly through the imino nitrogen atom, such species are unstable with respect to η^6–π coordination from the very electron-rich Dipp rings. By contrast, the monophosphaamidines form robust $LM(CO)_5$ complexes that are coordinated in the classical κ*P* coordination mode of phosphaalkenes, with an essentially planar ligand core oriented in-plane to the metal atoms and eclipsed with the CO ligands. Complexes **10–12** greatly expand on metal carbonyl complexes of "aminophosphaalkenes" of which there were previously only four structurally characterized in the literature (if **16** is included despite the double-substitution at C).[46–49] The P═C bond lengths of these coordinated species show the expected trends for electron-donating substituents delocalized into the highly polarizable heavy-element π bond. Coordination induces a significant bathochromic shift in the lowest absorption maxima. Semi-empirical and DFT calculations indicate that the destabilization of the HOMO is greater than that of the LUMO, resulting in a 3400 to 3500 cm^{-1} reduction in the energy of the allowed $\pi^* \leftarrow \pi$ transition upon coordination.

Group 6 carbonyl complexes have proven once again to be very useful "test-beds" for examining the properties of unsaturated main group compounds; in the work reported here, complexation is not essential for the preparation of the phosphaamidines which are electronically stabilized by nitrogen π donation,[27,29] but instead is necessary to select one of several solution-phase isomers and suppress the isomerization processes. Most importantly from the perspective of developing new phosphaamidinate coordination complexes,[6] the preparation of **10–12** provides assurances that the properties of "aminophosphaalkenes" bearing DippN groups – a moiety that has seen extensive use in chelating pincer ligand designs (such as NACNAC) – do not show the extreme changes in character as occurs with single or double substitution at C by the very powerful electron-donating NMe_2 groups as in **13** and **16**, especially when combined with strongly electron-withdrawing substituents as in **14** and **15**. Behaviour similar to amidinates can therefore be expected for anions derived from **9**.

Experimental

General

All experimental procedures were performed under a nitrogen atmosphere using modified Schlenk techniques. Metal carbonyls (Strem) were used as received. Solvents were reagent grade or better and used as received (methanol, ethanol, hexanes) or distilled over $LiAlH_4$ (*n*-heptane). Infrared spectra were recorded on a Bomem MB-100 or a Nicolet Avatar 360 spectrometer as KBr pellets or in a 0.1 mm NaCl solution cavity cell. ^1H, ^{31}P (without decoupling) and ^{13}C-$\{^1H\}$ NMR spectra were recorded on a Bruker AC250/Tecmag Macspect spectrometer operating at 250.13, 101.26 and 62.90 MHz, respectively, or a Varian INOVA 500 operating at 499.3, 202.1 and 125.6 MHz. ^1H NMR signals were referenced to tetramethylsilane, ^{13}P to external H_3PO_4, ^{13}C to $CDCl_3$. Electronic absorption spectra were obtained in 1 cm path-length Teflon-stoppered cuvettes on a Cary 1E spectrophotometer. Mass spectra analyses were undertaken in the Department of Chemistry, University of Alberta. Elemental analyses were performed by MHW Laboratories, Phoenix, Az. Phosphaamidines **9a,b** were produced as described elsewhere.[3,57] Solutions of $(THF)Cr,W(CO)_5$ were prepared by photolysis in THF solution and the reaction progress monitored by solution FTIR of aliquots.

Preparation of {1,3-bis(2,6-diisopropylphenyl)-2-(4-methylphenyl)-3-aza-1(λ^3,σ^2)-phosphapropene}-κ*P*-penta-carbonylchromium 10. In a 250 mL side arm flask, 0.500 g (1.06 mmol) phosphaamidine **9a** was combined with 125 mL of a 8.5×10^{-3} M $(THF)Cr(CO)_5$ solution in THF. The reaction was stirred for 1.5 hours and monitored by solution IR. No noticeable color change occurred. When the reaction was completed, THF was removed, leaving yellow solids. The solids were taken up in 90 mL of room temperature *n*-heptane, filtered through Celite™ and placed in a −15 °C freezer. Isolation of multiple crops gave 215 mg (0.324 mmol) of long needle-like yellow crystals, m.p. 180 °C (dec). Yield: 30.6%. X-ray data crystals were grown from a concentrated Et_2O solution cooled to −15 °C. Elemental Analysis: Calc. for $C_{37}H_{42}CrNO_5P$: C, 66.96; H 6.38, N 2.11%; found: C 67.12, H 6.18, N 2.05%. MS (70 eV): *m*/*z* 663.21879 (ML^+ based on ^{52}Cr, 0.31%); 607 ($ML - 2(CO)^+$, 1.6); 579 ($ML - 3(CO)^+$, 0.79); 523 ($ML - 5(CO)^+$, 67); 471 (L^+, 17); 428 ($L - {}^iPr^+$, 100); 278 ($L - C_6H_3{}^iPr_2PH^+$, 80); 105 ($C_8H_9^+$, 25); 91 ($C_7H_7^+$, 11). ^1H NMR ($CDCl_3$): δ 0.86 (d, J_{HH} = 6.6 Hz, 6H), 0.99 (d, J_{HH} = 6.7 Hz, 6H), 1.36 (d, J_{HH} = 6.7 Hz, 6H), 1.47 (d, J_{HH} = 6.7 Hz, 6H), 2.22 (d,

J(H–P) 1.8 Hz, 3H), 2.96 (sept., J_{HH} = 6.7 Hz, 2H), 4.00 (d of sept., J_{HH} = 6.7 Hz; J_{PH} = 4.6 Hz, 2H), 6.50 (s, 1H), 6.88 (d, J_{HH} 7.8 Hz, 2H), 6.92 (s, 4H), 7.05 (t, J_{HH} = 7.6 Hz, 1 H), 7.31 (d of d, J_{HH} = 7.9; J_{HP} = 2.4 Hz), 7.41 (t, J_{HH} = 7.9 Hz). ^{13}C NMR ($CDCl_3$): δ 21.4, 22.7 br, 24.8, 26.3 br, 26.6, 28.3, 34.3 (d, J_{CP} = 8.3 Hz), 123.6, 124.6 (d, J_{CP} = 4.9 Hz), 128.3, 128.8, 130.3 (d, J_{CP} = 13.7 Hz), 131.2 (d, J_{CP} = 2.9 Hz), 131.3 (d, J_{CP} = 23.4 Hz), 131.6, 134.4 (d, J_{CP} = 1.0 Hz), 139.7 (d, J_{CP} = 2.4 Hz), 146.8 (d, J_{CP} = 3.9 Hz), 158.2 (d, J_{CP} = 4.9 Hz), 189.9 P=*C* (d, J_{CP} = 5.4 Hz), 216.0 *C*O$_{eq}$ (d, J_{CP} = 15.1 Hz), 222.9 *C*O$_{ax}$ (d, J_{CP} = 4.9 Hz). ^{31}P NMR ($CDCl_3$): δ 45.03 ppm (s). IR (KBr pellet) cm^{-1}: 3358(w), 3054(w), 2966(w), 2927(w), 2870(w), 2069(s), 1955(vs), 1929(vs), 1907(vs), 1607(w), 1480(w), 1465(m), 1383(w), 1361(w), 1323(m), 1264(w), 1202(w), 1178(w), 815(w), 804(w), 759(w), 748(w) 607(m), 587(m).

Preparation of {1,3-bis(2,6-diisopropylphenyl)-2-(4-methylphenyl)-3-aza-(λ^3,σ^2)-phosphapropene}-κ*P*-penta-carbonylmolybdenum 11a. In a Schlenk tube, 0.500 g (1.06 mmol) of phosphaamidine **9a**, 0.280 g (1.06 mmol) $Mo(CO)_6$ and 26 mL of dry *n*-heptane were combined. The mixture was brought to reflux and periodically checked *via* solution IR of aliquots to monitor the consumption of metal carbonyl. After 8 hours heating was ceased and the solution was slowly cooled to −30 °C. After 6 days, the solution was filtered offering 0.284 g of fine yellow/brown crystals. Yield: 41%. Analytical crystals were grown by dissolving the crude crystals in room temperature heptane and cooling to −30 °C. Melting Point: 155 °C (decomp). Elemental Analysis: Calc. for $C_{37}H_{42}MoNO_6P$: C, 62.79; H, 6.00; N, 1.98. Found: C, 62.93; H, 6.15; N, 2.07%. MS (70 eV): *m*/*z* 709.18640 (ML$^+$ based on ^{98}Mo, 0.05%); 653 (ML − 2(CO)$^+$, 0.22); 625 (ML − 3(CO)$^+$, 1.1); 569 (ML − 5(CO)$^+$, 3.1); 471 (L$^+$, 15); 428 (L − ^{i}Pr$^+$, 100); 278 (L −$C_6H_3{}^iPr_2PH^+$, 67); 105 ($C_8H_9^+$, 18). ^{1}H NMR ($CDCl_3$): δ 0.79 (d, J_{HH} 6.7 Hz, 6H), 0.92 (d, J_{HH} 6.9 Hz, 6H), 1.29 (d, J_{HH} = 6.7 Hz, 6H), 1.40 (d, J_{HH} = 6.7 Hz, 6H), 2.15 (d, J_{HP} 1.8 Hz, 3H), 2.96 (sept., J_{HH} = 6.6 Hz, 2H), 3.91 (d of septet, J_{HH} = 6.7 Hz; J_{HH} = 4.6 Hz, 1H), 6.43 (s, 1H), 6.90 (d, J_{HH} 7.8 Hz, 2H), 6.99 (s, 4H), 7.07 (t, J_{HH} = 7.6 Hz, 1 H), 7.30 (d of d, J_{HH} = 7.9; J_{HP} = 2.4 Hz), 7.43 (t, J_{HH} = 7.9 Hz). ^{13}C NMR ($CDCl_3$): δ 21.3, 22.6 br, 24.5, 28.5 br, 26.3, 28.3, 34.1 (d, J_{CP} = 8.8 Hz), 123.7, 124.5 (d, J_{CP} = 4.9 Hz), 128.2, 128.2, 130.2 (d, J_{CP} = 14.2 Hz), 130.7 (d, J_{CP} = 24.4 Hz), 131.2, 131.3, 134.4, 139.7 (d, J_{CP} = 2.4 Hz), 146.4 (d, J_{CP} = 3.9 Hz), 154.2 (d, J_{CP} = 4.9 Hz), 187.9 P=*C* (d, J_{CP} = 5.4 Hz), 204.9 *C*O$_{eq}$ (d, J_{CP} = 10.7 Hz), 211.7 *C*O$_{ax}$ (d, J_{CP} = 30.8 Hz); some decomposition during data collection. ^{31}P NMR ($CDCl_3$): δ 30.17 ppm (s). IR (KBr pellet) cm^{-1}: 3362(w), 2963(w), 2927(w), 2869(w), 2061(s), 1994(m), 1986(m), 1946(vs), 1926(vs), 1913(vs), 1906(vs), 1461(w), 1384(w), 1363(w), 1321(w), 1204(w), 1108(w), 1056(w), 804(w)759(w), 748(w), 670(m), 656(m), 455(w).

Preparation of {1,3-bis(2,6-diisopropylphenyl)-2-(4-methoxylphenyl)-3-aza-(λ^3,σ^2)-phosphapropene}-κ*P*-penta-carbonylmolybdenum 11b. In a Schlenk tube, 0.140 g (0.530 mmol) $Mo(CO)_6$ and 0.258 g (0.530 mmol) phosphaamidine **9b** were combined with 13 mL *n*-heptane. The mixture was brought to reflux and the reaction progress monitored by solution IR. After 4 h, all of $Mo(CO)_6$ was consumed, leaving a dark green/yellow solution. Cooling to −30 °C yielded fine green/yellow needles. The crystals were then dissolved in 55 mL of room temperature heptane, filtered through Celite™ and cooled to −30 °C, giving small yellow blocks. Yield: 60 mg, 13.9%. mp: 150 °C (dec). Elemental Analysis: Calc. for $C_{37}H_{42}MoNO_6P$: C, 61.41; H, 5.85; N, 1.94. Found: C, 61.60; H, 5.93; N, 2.03%. MS (70 eV): *m*/*z* 741.19643 (M − 3(CO)$^+$ based on ^{98}Mo, 0.43%); 487 (L$^+$, 19); 444 (L − ^{i}Pr$^+$, 100); 326 (L − $C_6H_3{}^iPr_2^+$, 6); 294 (L − $C_6H_3{}^iPr_2PH^+$, 89); 121 ($C_8H_9O^+$, 22); 91 ($C_6H_5N^+$, 7). ^{1}H NMR ($CDCl_3$): δ 0.88 (d, J_{HH} = 6.7 Hz, 6H), 0.98 (d, J_{HH} = 6.9 Hz, 6H), 1.35 (d, J_{HH} = 6.7 Hz, 6H), 1.45 (d, J_{HH} = 6.7 Hz, 6H), 3.01 (sept., J_{HH} = 6.6 Hz, 2H), 3.71 (s, 3H), 4.00 (d of sept., J_{HH} = 6.7; J_{HH} = 4.7 Hz, 1H), 6.45 (s, 1H), 6.71 (d, J_{HH} 8.5 Hz, 2H), 6.91 (d, J_{HH} 7.8 Hz, 2H), 7.03 (d, J_{HH} = 7.8 Hz, 2H), 7.10 (t, J_{HH} = 7.6 Hz, 1 H), 7.30 (d of d, J_{HH} = 8.1; J_{HP} = 2.6 Hz), 7.44 (t, J_{HH} = 8.2 Hz). 6.690–7.47 (mult., 10H). ^{13}C NMR ($CDCl_3$): a reliable spectrum could not be obtained due to decomposition during data collection. ^{31}P NMR ($CDCl_3$): δ 29.55 ppm (s). IR (KBr) cm^{-1}: 3362(w), 3065(w), 2964(m), 2929(w), 2869(w), 2070(s), 1991(m), 1953(vs), 1933(vs), 1908(vs), 1606(w), 1575(w), 1511(w), 1459(m), 1384(w), 1363(w), 1324(w), 1296(w), 1253(m), 1207(w), 1174(w), 1107(w), 1040(w), 829(w), 804(w), 759(w), 606(m), 587(m).

Preparation of {1,3-bis(2,6-diisopropylphenyl)-2-(4-methylphenyl)-3-aza-(λ^3,σ^2)-phosphapropene}-κ*P*-penta-carbonyltungsten 12. In a 250 mL side arm flask, 0.500 g (1.06 mmol) phosphaamidine **9a** was combined with 125 mL of a 8.482 × 10^{-3} M (THF)$W(CO)_5$ solution in THF. A red solution formed which was allowed to stir overnight. Removal of THF left yellow-brown solids which were taken up in 65 mL of slightly warm *n*-heptane, filtered through Celite™ and placed in a −15 °C freezer. Isolation of multiple crops gave 208 mg (0.261 mmol) of yellow crystals, m.p. 170 °C (dec). Yield: 24.7%. Elemental Analysis: Calc. for $C_{37}H_{42}WNO_6P$: C, 55.85; H, 5.33; N, 1.76. Found: C, 56.03; H, 5.30; N, 1.79%. MS (70 eV): *m*/*z* 739.23915 (ML − 2(CO)$^+$ based on ^{184}W, 3.6%); 711 (ML − 3(CO)$^+$, 44); 683 (ML − 4(CO)$^+$, 2.1); 655 (ML − 5(CO)$^+$, 11); 471 (L$^+$, 12); 278 (L − $C_6H_3{}^iPr_2PH^+$, 100); 236 (L − $C_6H_3{}^iPr_2PH$ ^{i}Pr$^+$, 5.5); 222 ($C_8H_9NCC_6H_4CH_3^+$, 6); 105 ($C_8H_9^+$, 19); 91 ($CH_3C_6H_4^+$, 10). ^{1}H NMR ($CDCl_3$): δ 0.88 (d, J_{HH} = 6.7 Hz, 6H), 0.97 (d, J_{HH} = 6.7 Hz, 6H), 1.36 (d, J_{HH} = 6.7 Hz, 6H), 1.47 (d, J_{HH} = 6.7 Hz, 6H), 2.23 (d, J_{PH} 1.8 Hz, 3H), 3.02 (sept, J_{HH} = 6.8 Hz, 2H), 3.99 (d of sept, J_{HH} = 6.7 Hz; J_{PH} = 4.6 Hz, 1H), 6.45 (s, 1H), 6.91 (d, J_{HH} 7.6 Hz, 2H), 7.00 (s, 4H), 7.07 (t, J_{HH} = 7.7 Hz, 1 H), 7.32 (d of d, J_{HH} = 7.3; J_{HP} = 4.6 Hz), 7.45 (t, J_{HH} = 7.3 Hz). ^{13}C NMR ($CDCl_3$): a reliable spectrum could not be obtained due to decomposition during data collection. ^{31}P NMR ($CDCl_3$): δ 5.99 (d, $J(^{183}W–^{31}P)$ = 255 Hz). IR (KBr) cm^{-1}: 3357(w), 3055(w), 2966(m), 2927(w), 2871(w), 2067(s), 1979(s), 1946(vs), 1923(vs), 1901(vs), 1607(w), 1481(w), 1465(m), 1384(w), 1362(w), 1324(m), 1265(w), 1202(m), 1177(w), 816(w), 803(m), 759(w), 748(w), 597(m), 579(m), 512(w).

X-ray crystallography

Suitable crystals were selected and glued to a fine glass-fibre using epoxy resin. Data were collected on a Stoe IPDS image-

plate diffractometer system using Mo K_α radiation and a graphite monochromator. A ϕ-oscillation technique was employed to measure data at ambient temperature (the diffractometer was not equipped for low-temperature data collection). Data were corrected for Lorentz-polarization and either analytical or numerical (face-indexed) absorption corrections were applied. Data collection and post processing made use of the Stoe IPDS v2.36 software.[71] Structures were solved using direct methods within the SHELXTL suite of software; model refinement was undertaken in SHELX-2014.[72] In the case of **11b** and **12**, it was necessary to use a bond-distance constraint to obtain geometrically reasonable N–H distances. Displacement ellipsoids were high as expected for data collected at RT, particularly for pendant groups such as the *ortho*-^{i}Pr, and thus the enhanced rigid-bond restraints (RIGU) recommended for such cases were used.[73] The shape and size of the displacement ellipsoids for C42/O42 in **11b** were indicative of disorder; coupled to this was the apparent disorder in the backbone phenyl ring atoms C3/C4. A two-part disorder model was successfully refined with 65 : 35 occupancy ratios (see Fig. S6†). Attempts at refining ^{i}Pr group rotational disorder in all of these structures were judged to be unhelpful and a simple anisotropic refinement was adopted instead. Structures were visualized and illustrations were prepared using Mercury 3.5.[74] Crystal and experimental data are collected in Table S3 in the ESI.† Representations of the molecular structures are provided in Fig. 1–3 and S1, 2,† while selected interatomic distances and angles are provided in Table 1. Structure depositions: **9b**, CCDC 1421316; **10** 1421317; **11a**, 1421318; **11b**, 1421319; **10** 1421320 contain the supplementary crystallographic data for this paper.

Computation

Geometries for the computational studies were taken initially from the X-ray crystal structures. Calculations were performed using DFT at the B3PW91/LANL2DZ level of theory using Gaussian 03W.[75] The orbital energy interaction diagram was constructed using a combination of DFT and PM3 semi-empirical methods (the latter employing HyperChem release 8.0.10).[76] Calculations were deliberately restricted to the chromium examples to avoid having to deal with relativistic effects beyond the scope of this study. The geometry of **18** is taken from the deposited structure (CDC refcode MESTCR). Subsequently, full geometry optimizations were undertaken on **10** and **18** and the results were compared to those from the frozen geometries; the agreement was excellent. The geometries were confirmed to be at least local minima from the absence of imaginary frequencies in the full vibrational spectra calculations of the optimized structures. The Cartesian coordinates from these geometry-optimized calculations are provided in Tables S4 and S5,† and 3D structural pictures are shown in Fig. S4 and S7.†

Acknowledgements

We are indebted to Dr Gotthelf Wolmershäuser (Fachbereich Chemie der Universität Kaiserslautern, Erwin-Schrödinger-Straße, D-67663 Kaiserslautern, Germany) for collecting all the X-ray diffraction data. Financial support of this work by the Natural Sciences and Engineering Research Council of Canada and the University of Lethbridge is gratefully acknowledged. We thank a referee for the suggestion of refining a disorder model for **11b**.

Notes and references

1 K. Issleib and O. Löw, *Z. Anorg. Allg. Chem.*, 1966, **346**, 241–254. The title of this paper "P-substituted acid phosphides RCO-PR′$_2$ and phosphamidines RC(NR)-PR′$_2$" indicates a deliberate effort to replace a nitrogen with a phosphorus in amides and amidines.
2 K. Issleib, H. Schmidt and H. Meyer, *J. Organomet. Chem.*, 1978, **160**, 47–57. In this, the first study reporting on *N*,*P*-disubstituted (and hence potentially ionisable) derivatives, their terminology shifts to "phosphaamidine".
3 R. T. Boeré, M. L. Cole, P. C. Junk, J. D. Masuda and G. Wolmershäuser, *Chem. Commun.*, 2004, 2564–2565.
4 M. Song, B. Donnadieu, M. Soleilhavoup and G. Bertrand, *Chem. – Asian J.*, 2007, **2**, 904–908. See references therein for a reasonably comprehensive survey of the background.
5 X. Li, H. Song and C. Cui, *Dalton Trans.*, 2009, 9728–9730.
6 T. van Dijk, S. Burck, M. K. Rong, A. J. Rosenthal, M. Nieger, J. C. Slootweg and K. Lammertsma, *Angew. Chem., Int. Ed.*, 2014, **53**, 9068–9071.
7 S. N. MacMillan, J. M. Tanski and R. Waterman, *Chem. Commun.*, 2007, 4172–4174.
8 A. J. Roering, S. E. Leshinski, S. M. Chan, T. Shalumova, S. N. MacMillan, J. M. Tanski and R. Waterman, *Organometallics*, 2010, **29**, 2557–2565.
9 A. J. Roering, L. T. Elrod, J. K. Pagano, S. L. Guillot, S. M. Chan, J. M. Tanskib and R. Waterman, *Dalton Trans.*, 2013, **42**, 1159–1167.
10 A. F. Maddox, J. J. Davidson, T. Shalumova, J. M. Tanski and R. Waterman, *Inorg. Chem.*, 2013, **52**, 7811–7816.
11 M. Westerhausen and M. H. Digeser, *Inorg. Chem.*, 1997, **36**, 521–527.
12 M. Westerhausen and M. H. Digeser, *Z. Anorg. Allg. Chem.*, 1997, **623**, 1237–1242.
13 P. Le Floch, *Coord. Chem. Rev.*, 2006, **250**, 627–681.
14 J. D. Protasiewicz, Multiply bonded compounds of Group 15 elements, in *Comprehensive Inorganic Chemistry II*, Elsevier, 2013, pp. 325–348.
15 R. C. Fischer and P. P. Power, *Chem. Rev.*, 2010, **110**, 3877–3923.
16 N. C. Norman, *Polyhedron*, 1993, **12**, 2431–2466.
17 A. N. Chernega, M. Yu. Antipin and Yu. T. Struchkov, *J. Struct. Chem.*, 1988, **29**, 265–303.
18 J. F. Nixon, *Chem. Rev.*, 1988, **88**, 1327–1362.

19 M. Klein, C. Albrecht, G. Schnakenburg and R. Streubel, *Organometallics*, 2013, **32**, 4938–4943.
20 C. Albrecht, L. Shi, J. M. Pérez, M. van Gastel, S. Schwieger, F. Neese and R. Streubel, *Chem. – Eur. J.*, 2012, **18**, 9780–9783.
21 S. Ito, S. Kimura and M. Yoshifuji, *Chem. Lett.*, 2002, 708–709.
22 T. W. Mackewitz, D. Ullrich, U. Bergsträsser, S. Leininger and M. Regitz, *Liebigs Ann.*, 1997, 1827–1839.
23 M. Hobbold, R. Streubel, M. H. A. Benvenutti, P. B. Hitchcock and J. F. Nixon, *Organometallics*, 1997, **16**, 3726–3728.
24 R. Streubel, M. Hobbold, J. Jeske and P. G. Jones, *Angew. Chem., Int. Ed. Engl.*, 1997, **36**, 1095–1097.
25 L. Weber, I. Schumann, H.-G. Stammler and B. Neumann, *Chem. Ber.*, 1994, **127**, 1349–1353.
26 E. Fuchs, B. Breit, H. Heydt, W. Schoeller, T. Busch, C. Kruger, P. Betz and M. Regitz, *Chem. Ber.*, 1991, **124**, 2843–2855.
27 A. Marinetti, S. Bauer, L. Ricard and F. Mathey, *J. Chem. Soc., Dalton Trans.*, 1991, 597–602.
28 L. Weber, E. Lücke, A. Müller and H. Bögge, *Z. Anorg. Allg. Chem.*, 1990, **583**, 91–101.
29 A. Marinetti, S. Bauer, L. Ricard and F. Mathey, *Organometallics*, 1990, **9**, 793–798.
30 B. A. Boyd, R. J. Thoma, W. H. Watson and R. H. Neilson, *Organometallics*, 1988, **7**, 572–574.
31 T. C. Klebach, R. Lourens, F. Bickelhaupt, C. H. Stam and A. van Herk, *J. Organomet. Chem.*, 1981, **210**, 211–221.
32 A. Özbolat-Schön, M. Bode, G. Schnakenburg, A. Anoop, M. van Gastel, F. Neese and R. Streubel, *Angew. Chem., Int. Ed.*, 2010, **49**, 6894–6898.
33 J. Escudié and H. Ranaivonjatovo, *Organometallics*, 2007, **26**, 1542–1559.
34 S. Ito, S. Kimura and M. Yoshifuji, *Org. Lett.*, 2003, **5**, 1111–1114.
35 K. Toyota, S. Kawasaki and M. Yoshifuji, *Tetrahedron Lett.*, 2002, **43**, 7953–7959.
36 S. Ito, K. Toyota and M. Yoshifuji, *J. Organomet. Chem.*, 1998, **553**, 135–140.
37 M. Yoshifuji, K. Toyota, T. Uesugi, I. Miyahara and K. Hirotsu, *J. Organomet. Chem.*, 1993, **461**, 81–84.
38 M. Nieger, N. Siabalis and R. Appel, *Z. Kristallogr.*, 1993, **206**, 295–297.
39 M. Yoshifuji, K. Toyota, T. Niitsu, N. Inamoto and K. Hirotsu, *J. Organomet. Chem.*, 1990, **389**, C12–C15.
40 M. Yoshifuji, K. Toyota, T. Sato, N. Inamoto and K. Hirotsu, *Heteroat. Chem.*, 1990, **1**, 339–342.
41 V. Nesterov, L. Duan, G. Schnakenburg and R. Streubel, *Eur. J. Inorg. Chem.*, 2011, 567–572.
42 S. Ito, S. Kimura and M. Yoshifuji, *Bull. Chem. Soc. Jpn.*, 2003, **76**, 405–412.
43 L. Weber, M. Meyer, H.-G. Stammler and B. Neumann, *Chem. – Eur. J.*, 2001, **7**, 5401–5408.
44 L. Weber, B. Quasdorff, H.-G. Stammler and B. Neumann, *Chem. – Eur. J.*, 1998, **4**, 469–475.
45 L. Boubekeur, L. Ricard, P. Le Floch and N. Mézailles, *Organometallics*, 2005, **24**, 3856–3863.
46 L. Weber, M. Meyer, H.-G. Stammler and B. Neumann, *Organometallics*, 2003, **22**, 5063–5068.
47 J. Grobe, D. Le Van, U. Althoff, B. Krebs, M. Dartmann and R. Gleiter, *Heteroat. Chem.*, 1991, **2**, 385–394.
48 J. Grobe, D. Le Van, J. Nientiedt, B. Krebs and M. Dartmann, *Chem. Ber.*, 1988, **121**, 655–664.
49 L. Weber, S. Uthmann, H.-G. Stammler, B. Neumann, W. W. Schoeller, R. Boese and D. Blaser, *Eur. J. Inorg. Chem.*, 1999, 2369–2381.
50 L. Weber, *Eur. J. Inorg. Chem.*, 2005, 4590–4597.
51 W. W. Schoeller, A. B. Rozhenko and S. Grigoleit, *Eur. J. Inorg. Chem.*, 2001, 2891–2898.
52 J. B. Barker and M. Kilner, *Coord. Chem. Rev.*, 1994, **133**, 219–300.
53 R. T. Boeré, V. Klassen and G. Wolmershäuser, *J. Chem. Soc., Dalton Trans.*, 1998, 4147–4154.
54 R. T. Boeré, V. Klassen and G. Wolmershäuser, *Can. J. Chem.*, 2000, **78**, 583–589.
55 M. P. Coles, *Dalton Trans.*, 2006, 985–1001.
56 F. A. Cotton, T. Inglis, M. Kilner and T. R. Webb, *Inorg. Chem.*, 1975, **14**, 2023–2026.
57 J. D. Masuda, L. Mokhtabad Amrei and R. T. Boeré, in preparation.
58 G. Wilkinson, R. D. Gillard and J. A. McCleverty, *Comprehensive Coordination Chemistry*, Pergamon Press, New York, 1st edn, 1987.
59 F. H. Allen, *Acta Crystallogr., Sect. B: Struct. Sci.*, 2002, **58**, 380–388.
60 J. Dugal-Tessier, E. D. Conrad, G. R. Dake and D. P. Gates, Phosphaalkenes, in *Phosphorus(III) Ligands in Homogeneous catalysis: design and synthesis*, ed. P. C. J. Kamer and P. W. N. N. van Leeuwen, Wiley, 2012, p. 239.
61 M. Yoshifuji, K. Shibayama, T. Hashida, K. Toyota, T. Niitsu, I. Matsuda, T. Sato and N. Inamoto, *J. Organomet. Chem.*, 1986, **311**, C63–C67.
62 P. S. Pregosin and R. W. Kunz, *^{31}P and ^{13}C NMR of transition metal phosphine complexes*, Springer-Verlag, Berlin, 1979.
63 R. L. Keiter and J. G. Verkade, *Inorg. Chem.*, 1969, **8**, 2115–2120.
64 G. M. Bodner, *Inorg. Chem.*, 1975, **14**, 2694–2699.
65 İ. A. Mour, S. Ozkar and C. G. Kreiter, *Z. Naturforsch.*, 1994, **49b**, 1059–1062.
66 D. S. Braterman, *Metal Carbonyl Spectra*, Academic Press, New York, 1975.
67 J. Deberitz and H. Nöth, *J. Organomet. Chem.*, 1973, **49**, 453–467.
68 M. Yoshifuji, K. Toyota and N. Inamato, *Tetrahedron Lett.*, 1985, **26**, 1727–1730.
69 M. T. Nguyen, M. A. McGinn and A. F. Hegarty, *Polyhedron*, 1986, **5**, 1223–1226.
70 J. Grobe, D. Le Van, B. Krebs, R. Fröhlich and A. Schiemann, *J. Organomet. Chem.*, 1990, **389**, C29–C33.
71 STOE & Cie GmbH, Darmstadt 64295 Germany.

72 G. M. Sheldrick, *Acta Crystallogr., Sect. C: Cryst. Struct. Commun.*, 2015, **71**, 3–8.
73 A. Thorn, B. Dittrich and G. M. Sheldrick, *Acta Crystallogr., Sect. A: Fundam. Crystallogr.*, 2012, **68**, 448–451.
74 C. F. Macrae, I. J. Bruno, J. A. Chisholm, P. R. Edgington, P. McCabe, E. Pidcock, L. Rodriguez-Monge, R. Taylor, J. van de Streek and P. A. Wood, *J. Appl. Crystallogr.*, 2008, **41**, 466–470.
75 M. J. Frisch, G. W. Trucks, H. B. Schlegel, G. E. Scuseria, M. A. Robb, J. R. Cheeseman, J. A. Montgomery Jr., T. Vreven, K. N. Kudin, J. C. Burant, J. M. Millam, S. S. Iyengar, J. Tomasi, V. Barone, B. Mennucci, M. Cossi, G. Scalmani, N. Rega, G. A. Petersson, H. Nakatsuji, M. Hada, M. Ehara, K. Toyota, R. Fukuda, J. Hasegawa, M. Ishida, T. Nakajima, Y. Honda, O. Kitao, H. Nakai, M. Klene, X. Li, J. E. Knox, H. P. Hratchian, J. B. Cross, V. Bakken, C. Adamo, J. Jaramillo, R. Gomperts, R. E. Stratmann, O. Yazyev, A. J. Austin, R. Cammi, C. Pomelli, J. W. Ochterski, P. Y. Ayala, K. Morokuma, G. A. Voth, P. Salvador, J. J. Dannenberg, V. G. Zakrzewski, S. Dapprich, A. D. Daniels, M. C. Strain, O. Farkas, D. K. Malick, A. D. Rabuck, K. Raghavachari, J. B. Foresman, J. V. Ortiz, Q. Cui, A. G. Baboul, S. Clifford, J. Cioslowski, B. B. Stefanov, G. Liu, A. Liashenko, P. Piskorz, I. Komaromi, R. L. Martin, D. J. Fox, T. Keith, M. A. Al-Laham, C. Y. Peng, A. Nanayakkara, M. Challacombe, P. M. W. Gill, B. Johnson, W. Chen, M. W. Wong, C. Gonzalez and J. A. Pople, *Gaussian 03, Revision C.02*, Gaussian, Inc., Wallingford CT, 2004.
76 *HyperChem™ Release 8.0.10 for Windows*, Hypercube Inc., 1995–2011.
77 N. Nebra, C. Lescot, P. Dauban, S. Mallet-Ladeira, B. Martin-Vaca and D. Bourissou, *Eur. J. Org. Chem.*, 2013, 984–990.